Construction and Building Materials 61 (2014) 230–240

Contents lists available at ScienceDirect

Construction and Building Materials

journal homepage: www.elsevier.com/locate/conbuildmat

Bond behavior of steel and GFRP bars in self-compacting concrete

Emadaldin Mohammadi Golafshani, Alireza Rahai *, Mohammad Hassan Sebt

Department of Civil and Environmental Engineering, Amirkabir University of Technology, Tehran, Iran

HIGHLIGHTS

- Investigation of bond behavior of GFRP bars in SCC.
- Comparison of bond behavior of GFRP bars with Steel ones in SCC.
- Variations of bond strength of GFRP bars in vertical and horizontal SCC specimens.
- Comparison of bond behavior of GFRP bars with Steel ones in vertical and horizontal SCC specimens.
- Comparison of available codes and equations regarding to the prediction of bond strength.

ARTICLE INFO

Article history:
Received 1 July 2012
Received in revised form 9 February 2014
Accepted 11 February 2014

Keywords:
Bond behavior
GFRP bar
Pullout
Self-compacting concrete

ABSTRACT

The bond behavior of steel and GFRP bars in concrete is one of the most important issues in reinforced concrete structures and depends on several factors, such as the structural characteristics, bar and concrete properties. Self-compacting concrete (SCC) is a highly flowable, non-segregation concrete that spreads into place, fills formwork, and moves between even the most congested reinforcement, all without any mechanical vibration. In order to investigate the effect of bleeding, statistical and dynamical segregation on the bond behavior of steel and GFRP bars in SCC, two types of vertical and horizontal concrete elements with four bars located at different positions were built and the bond behaviors of the above mentioned bars in two types of SCC were investigated and compared with that of normal concrete (NC).

The results revealed that regarding the suitable adhesion treatment of steel bars, their bond behavior is higher than that of GFRP bars in SCC. The drop in bond strength of steel bars at the top of vertical elements averages 5.49% less in SCC than in NC and 8.06% in the case of GFRP bars. Also, for both SCC and NC, reducing the water to cement ratio and using high powdery materials decreases the bond strength variations in horizontal and vertical elements. However, the bond strength variations of steel bars are less than that of GFRP bars.

1. Introduction

Several new materials are being developed for construction projects especially in the last three decades. High strength and stiffness, light weight, long service life, and low assembly and maintenance costs are some qualitative performance advantages of these new materials compared to conventional ones. High performance materials such as self-compacting concrete (SCC) and fiber reinforced polymer reinforcement (FRP) are a few of the construction materials being used in innovative ways that are technically viable substitutes for conventional materials.

Self-compacting concrete (SCC), a new special type of concrete mixture, is defined as a concrete that has excellent deformability and high resistance to segregation and can be filled in heavily reinforced or restricted areas without applying vibration. SCC was developed in Japan [1] in the late 1980s and recently, this material has gained wide use in many countries for different applications and structural configurations [2–10].

Another new material that has the potential to show up on the construction industry market is Fiber Reinforced Polymer (FRP) reinforcement. FRP bars have become very attractive in the field of reinforced concrete structures as a new construction material. The success of FRP bars is mainly linked to their high mechanical performances, low weight, satisfactory durability in an aggressive environment and tailorability [11].

In order to enhance the application of FRP bars in civil engineering projects, all aspects of their structural behavior must be studied further to assure their performance. The bond between concrete and reinforcing bars is important to the structural integrity and

* Corresponding author. Tel.: +98 2166468055; fax: +98 2166497921.
E-mail address: a_rahai@yahoo.com (A. Rahai).

http://dx.doi.org/10.1016/j.conbuildmat.2014.02.021
0950-0618/© 2014 Elsevier Ltd. All rights reserved.

durability of a reinforced concrete structural member. The bond stress transferred between reinforcing bars and the surrounding concrete is made up of three components: chemical adhesion, friction resistance, and mechanical interaction between the ribs of the bar and the surrounding concrete. Bond failure of bars normally involves the following phenomena [12]: (1) local crushing of concrete in front of the bar ribs, and/or (2) splitting of the concrete due to radial cracks around the bar. Local crushing dominates when the confinement provided by either surrounding concrete or transverse reinforcement is large and/or the rib height is small. This mechanism of bond failure tends to be ductile. Splitting of the concrete dominates when the confinement is small and/or the rib height is large and this mechanism is brittle.

Compared to steel bars, the bond of FRP bars depend on a greater number of factors. Moreover, the types of FRP bars are numerous. Their surface is weaker than that of steel bars and may be fractured by bond forces [13]. Also, in the cases of SCC, the differences in the mixture design with respect to NC cause a completely different internal structure characterized by a denser interfacial transition zone (ITZ) and homogeneously distributed fine voids. Due to the microstructure differences between SCC and NC, the bond performance is expected to differ in the two cases [14–18].

Lots of efforts have been made to investigate the bond mechanism of steel bars in SCC, with particular reference to the pullout behavior and the so-called "top bar effect". Some authors have reported that the bond strength of steel bars does not change with the location of the bars along the height of a concrete member cast with SCC, but the tests were carried out on specimens that were only 300 mm high and with compressive strength higher than 50 MPa [19]. Tests made on taller specimens have revealed that there are in fact losses of bond strength with height, although the results obtained do not always agree. Generally, a more uniform behavior is registered in the SCCs [5,20,21]. Khayat et al. [5] reported that the top-bar factor for reinforcing steel bars positioned approximately at 1.4 m from the bottom of a wall varied between approximately 1.3 and 1.6 for the SCC compared to 2.0 for the NC. Valcuende and Parra [22] revealed that in vertically cast pieces, depending on the mix, the loss in mean bond strength between the upper and lower areas of 1.5 m tall columns varies by between 40% and 61% in SCC and between 70% and 86% in NC. Furthermore, viscosity agents were found to enhance the stability of fresh SCC and reduce the top-bar effect [14,23]. On the contrary, Esfahani et al. [24] point out that losses of bond at the top of 900 mm high walls are 20% greater in SCC mixes, and propose an increase of 30% in the factor that takes into account the top-bar effect in calculating the anchorage length for this type of concrete. Nevertheless, it must be stated that the authors used a small concrete cover of the reinforcing bars in these tests, which caused a premature failure of the bond due to splitting of concrete, and resulted in a wide scatter of results.

Many studies have been conducted to investigate the interfacial bond behavior of FRP bars in normal and high strength concrete. The bond strength of FRP bars (with surface deformations) is typically within 40–100% of that corresponding to steel bars [25]. Smooth bars develop only 10–20% of bond strength of deformed bars. Surface deformations with a height of at least 6% of the bar diameter are necessary to develop adequate bond behavior to concrete. Square bars develop more superior bond strength than round bars due to a more pronounced wedging effect [26]. Larger diameter bars develop less bond strength possibly due to more shear lag and Poisson effect [26,27]. The average bond strength decreases with the increase of embedment length due to the nonlinear bond stress distribution along the bar [26,27]. The bond strength is lower when the bar has more than 305 mm of concrete cover below, due to the upward migration of air, water and fine particles during casting [28]. Due to its low modulus of elasticity, the slip of FRP bar relative to the surrounding concrete is greater than that of steel bars and unlike steel bars, the post peak bond strength of FRP bars significantly affects the calculation of the development length [27]. The interfacial bond strength of GFRP bars increased as the compressive strength of concrete increased. However the increasing rate of the bond strength of the GFRP bars with respect to the concrete strength was much smaller than that of the steel bars [29]. Bond strength reduction of CFRP bars is lower compared to GFRP bars in different environmental conditions [30]. The bond strength of GFRP bars in concrete exhibited a severe reduction of 80–90% at a relatively low temperature (up to 200 °C) [31]. The bond strength of the FRP bar in concrete was enhanced by 5–70% as the volume fraction of fiber increased [32].

However, limited research has been carried out to study the bond behavior of GFRP bars in SCC. This paper describes pullout tests and compares the bond strength of steel and GFRP bars in SCC and NC. The variation of bond strength along the height (for vertical casting) and along the horizontal distance (for horizontal casting) of pullout specimens is compared for both steel and GFRP bars taking into account the compressive strength and top-bar effect.

2. Experimental program

2.1. Materials

2.1.1. Reinforcing bars

One type of GFRP and steel bar supplied by international manufacturers were used in this study. The GFRP bar used in this research is made of continuous longitudinal glass fibers glued together with a thermosetting resin and was manufactured using the pultrusion process. The nominal diameter of the GFRP and steel bars was 16 mm. The type of steel and GFRP ribbed bars are shown in Fig. 1 and their properties are shown in Table 1.

2.1.2. Cementitious material

In this study, ASTM Type I Portland cement (PC) and silica fume with specific gravity of 3.14 and 2.14 were used, respectively. Chemical compositions of cementitious materials are presented in Table 2.

2.1.3. Aggregates

12-mm maximum size crushed limestone and natural sand were used as coarse and fine aggregate, respectively. The coarse and fine aggregates each had a specific gravity of 2.56 and 2.54 and water absorptions of 2.11% and 2.45%, respectively. Also, silica powder with a gravity of 2.72 was used as filler.

2.1.4. Chemical admixtures

Glenium 110P with specific gravity of 1.06 was used as a superplasticizer (SP) in concrete mixtures. This type of superplasticizer produces air bubbles in concrete.

2.2. Concrete mix proportions

Two SCC and NC mixtures consisting of different components were used. The mix proportions of all four concrete mixtures are summarized in Table 3. For all SCC mixtures, the content of the silica fume was generally maintained at about

Fig. 1. Surface deformation of steel and GFRP bars.

Table 1
Material properties of bars.

Bars	Nominal diameter (mm)	Fiber content (%)	f_y (MPa)	f_u (MPa)	E_s (GPa)
Steel	16	–	425	560	213
GFRP	16	0.7	1050	–	61

Table 2
The chemical properties of cement (% by mass).

Compositions	SiO_2	Al_2O_3	Fe_2O_3	CaO	SO_3	MgO	Na_2O	K_2O	P_2O_5	TiO_2	LOI
Cement type I	21.5	3.68	2.76	61.5	2.5	4.8	0.12	0.95	0.23	0.04	1.35
Silica fume	95.1	0.6	1.1	1.02	1.2	0.6	–	–	–	–	–

Table 3
The mix proportions of concrete mixtures.

Concrete type	Cement	Silica fume	Coarse aggregate	Fine aggregate	Silica powder	Free water	Water to binder ratio	SP (% mass of cement)
SCC1	350	35	615	922	200	173	0.45	0.7
SCC2	450	45	597	895	150	173	0.35	1
NC1	400	0	910	910	0	160	0.40	0.1
NC2	500	0	882	882	0	150	0.30	0.4

All dimensions are in kg.

10% cement in the mix design. The proportion of the aggregate used for SCC was 60% sand and 40% coarse aggregate by the total weight of the aggregate and 50% sand and 50% coarse aggregate by the total weight of the aggregate for NC.

2.3. Concrete casting

In the production of SCC mixtures, the mixing sequence and duration are important and effective, so the procedure for batching and mixing proposed by Khayat et al. [33] was employed to supply the same homogeneity and uniformity in all mixtures. The batching sequence consisted of homogenizing the fine and coarse aggregates for 30 s in a rotary planetary mixer with a speed of 25 rpm, then adding about half of the water into the mixer and continuing to mix for one more minute. Thereafter, the aggregates were left to absorb the water in the mixer for 1 min. Then cement and mineral additives were added, the mixing was resumed for another minute. Finally, the SP with the remaining water was introduced, and the concrete was mixed for 3 min and then left for 2 min to rest. Eventually, the concrete was mixed for an additional two minutes to complete the mixing sequence. Then the tests were conducted on the fresh concrete to determine the slump flow diameter [34], the V-funnel flow time [35], the L-box height ratio [3] and the segregation ratio in terms of segregation index (SI) [36].

To determine the compressive strength of concrete, three 150 mm cubes were taken from each concrete mixture. The SCC specimens were cast without any compaction and vibration, whereas NC specimens were placed in three layers of approximately equal thickness and each layer was rodded 25 times with a 16 mm diameter tamping rod. After 24 h casting, they were demoulded and stored in lime saturated water until the testing date on the 28th day. The results of fresh and hardened properties of SCC and NC are listed in Table 4.

2.4. Pull out test program

2.4.1. Preparation of specimens

Fig. 2 shows the schematic sketch of 1400 mm × 200 mm × 200 mm pullout specimens with four 16 mm diameter deformed reinforcing bars. All the bars were 650 mm long, with a 48 mm contact with concrete and centric bar placement. In order to control the bond length, the bar was prepared with a bond breaker, which consisted of soft plastic tubing inserted around the bar to prevent their contact. The test specimens were classified in two series. Series (a) that were cast horizontally in the form of beam configuration and Series (b) that were cast vertically in the form of column one. The effect of the location of horizontal reinforcing bars on the bond behavior of steel and GFRP bars over the height of a vertical element in NC and SCC was studied in series (a) specimens. Also, the effect of filling ability and dynamic segregation of SCC on the bond strength of bars in SCC was investigated in series (b) specimens. For each sample, the pullout test was carried out perpendicularly to the casting direction. Two batches were made for each mix and two beams and columns were fabricated from each of them. The NC specimens were placed in three layers of approximately equal thickness and each layer was compacted by a mechanical vibrator whereas the SCC specimens were cast full without any compaction and vibration. After 24 h casting, as shown in Fig. 3, the specimens were demoulded and stored in lime saturated water until the date of testing on the 28th day. After this time, the specimens were sawn to obtain 200 mm cube specimens for the pullout test.

2.4.2. Test setup and instrumentation

The setup for the pullout test is shown in Fig. 4. The tests were performed using the universal material testing machine with a capacity of 1000 kN. A loading frame mounted in the lower position of the machine by means of four high strength bolts, was used to transfer the reaction from the specimen to the machine. There was a 15 mm wooden plate placed between the concrete specimen and supporting steel block to prevent bending or movement due to the irregularities at the contact surface of the specimen during loading. The load was applied to the bar at a rate of 0.02 mm/s. Hence, all the tests were carried out in displacement control mode so as to obtain the post peak behavior and the load was measured with an electronic load cell of the machine.

3. Results and discussion

The results of 104 cube tests are used to evaluate the bond behavior of steel and GFRP bars in NC and SCC. The general coding notation applied for bars embedded in concrete is as follows:

1. The first number of the code indicates the concrete cube compressive strength in MPa;
2. The first letter denotes the type of concrete (NC and SCC);

Table 4
The results of fresh and hardened properties of SCC and NC.

Concrete type	Slump flow* (mm)	T500 (s)	V-funnel (s)	L-box ratio (%)	J-ring (mm)	Segregation resistance (%)	U-Box Difference (mm)	28 day f_{cu} (MPa)
SCC1	720	2.6	7.6	>80%	<10 mm	<10%	<30 mm	44.88
SCC2	680	3.9	11.7	>80%	<10 mm	<10%	<30 mm	59.77
NC1	80–100	–	–	–	–	–	–	47.98
NC2	80–100	–	–	–	–	–	–	64.65

* In the case of normal concrete, the Abrams' slump was stated.

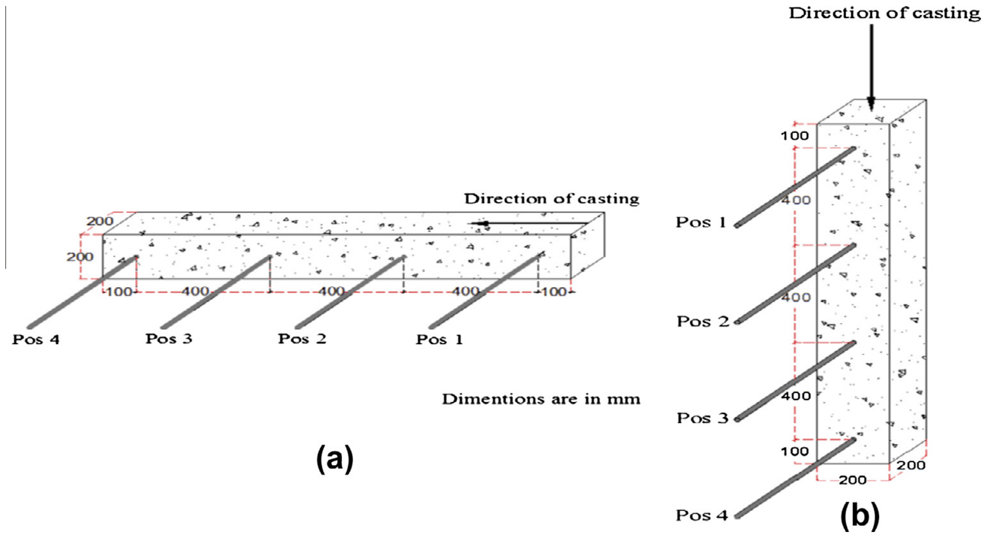

Fig. 2. Schematic sketch of specimens: (a) horizontal casting, (b) vertical casting.

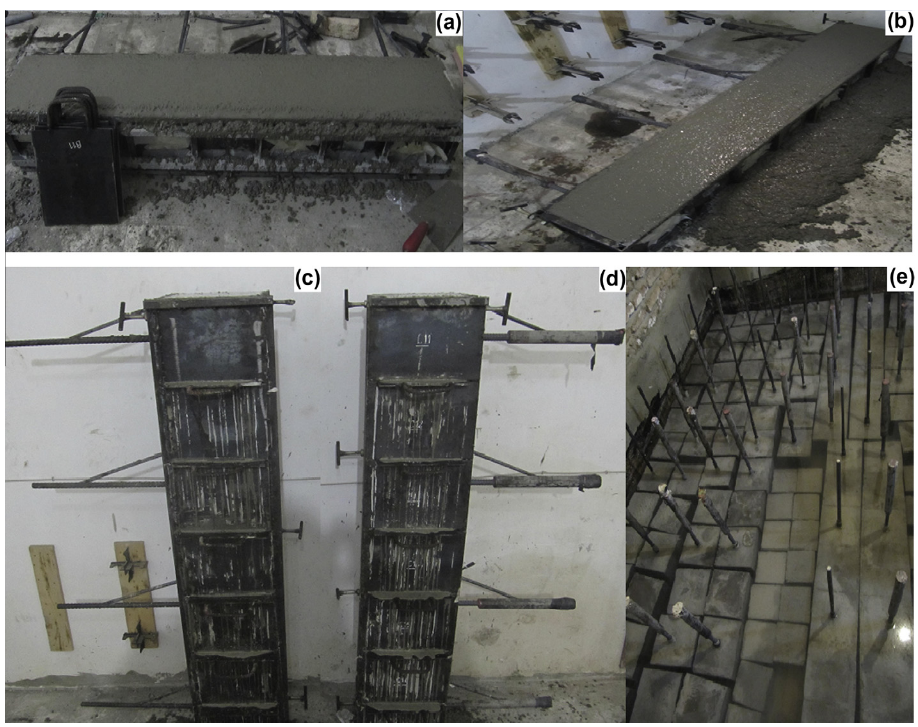

Fig. 3. Setup for fabrication of specimens (a) steel, (b) GFRP bars in beam shape forms, (c) steel, (d) GFRP bars in column shape forms and (e) curing of specimens.

3. The second letter denotes the kind of reinforcing bar used in the test (St for steel and Gr for GFRP bar);
4. The next letter denotes the type of specimens (V for vertically, H for horizontally and N for normal specimens).
5. The second number indicates the position of bars in specimens (P1, P2, P3 and P4 for position 1, position 2, position 3, and position 4, respectively).

For example, 48-N-St-V-P3 designates a steel bar in position 3 of a vertical formwork cast in NC with a compressive strength of 48 MPa.

The bond strength was calculated assuming a uniform distribution of bond stresses along the bond length. It was calculated from the ultimate pull-out load using Eq. (1).

$$\tau_b = \frac{F_u}{\pi \cdot l_d d_b} \tag{1}$$

where τ_b is the ultimate bond strength (MPa), d_b is the bar diameter (mm), l_d is the bond length (mm) and F_u is the ultimate pull-out load (kN).

To compare the bond strength of SCCs and NC, the variation of compressive strength has to be taken into account. The bond strength is normalized by dividing it by $\sqrt{f_{cu}}$, which is the criterion found often in the literature [37].

$$\tau_R = \tau_b / \sqrt{f_{cu}} \tag{2}$$

where τ_R is the normalized bond strength and f_{cu} is the compressive strength of concrete. The results are listed in Table 5.

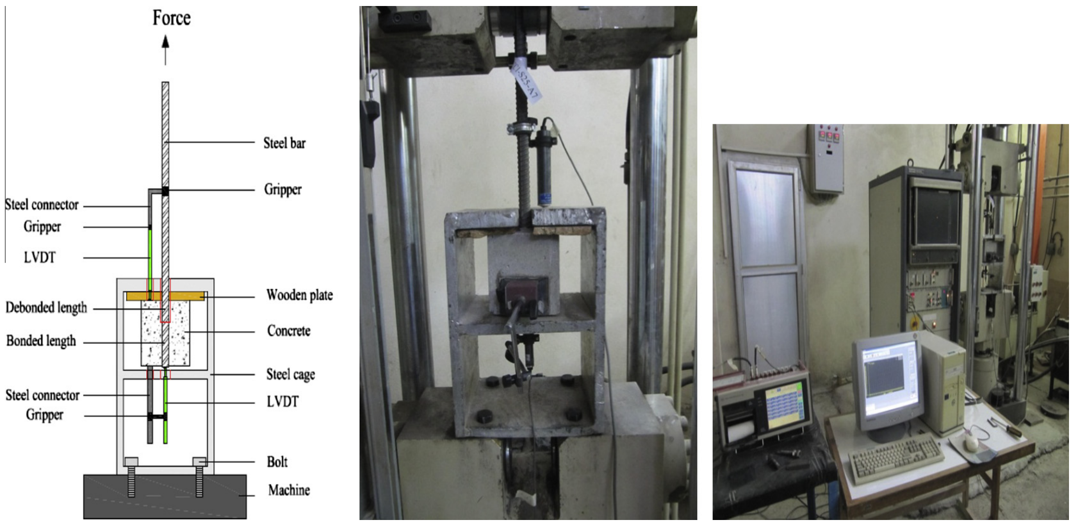

Fig. 4. The setup for the pullout test and monitoring of experiment.

3.1. Bond stress–slip relationship curves

Fig. 5 shows the bond stress of steel and GFRP bars in NC and SCC related to the free end slip. In this investigation, the form of bond stress–slip relationship did not show significant difference between NC and SCC mixes and steel and GFRP bars. At the beginning of loading, no measurable slip was observed and it was attributed to the chemical adhesion between the bars and concrete. Analyzing the figures shows that for both steel and GFRP bars, their chemical adhesion in SCC is higher than NC. This could be related to the better filling ability and higher powdery materials of SCC compared to NC. Also, for both NC and SCC, the chemical adhesion of steel bars is higher than GFRP bars. This is because of the better surface treatment of steel bars compared to GFRP ones in concrete. In the second stage, up to maximum bond stress, the bond between bars and concrete is due to the mechanical interlocking. In this stage, the microcracks of concrete propagate from the front of the bar deformation to the cover of concrete. If the cracking reaches the cover of concrete, the failure mechanism is splitting and otherwise the pullout mechanism occurs Pullout failure occurs once the shear strength of the bond between the bar and the concrete is exceeded. If the cracking does not reach the cover of concrete, the peak stress is reached, the slip increases and the load decreases; At this stage, mechanical contribution is progressively reduced and finally the friction through wedging of the bar deformation on the surrounding concrete becomes the predominant bond mechanism. However, in this study, some specimens failed by pullout of the bars and some others by splitting of the enclosing concrete. The bond strength and the failure mechanism of specimens are shown in Table 5.

The failure mechanisms of some steel and GFRP bars in NC and SCC are shown in Fig. 6. The investigations reveal that, in the case of steel bars, ultimate bond failure occurs due to concrete crushing against the bar deformation. For NC and SCC, increasing the level of bond stress caused the pullout failure mechanism to convert to a splitting failure. The reason is the higher propagation of cracking

Table 5
Mechanical properties and pullout test results.

Specimens	f_{cu} (MPa)	τ_b (MPa)	$\tau_R(\sqrt{\text{MPa}})$	Mode of failure	Specimens	f_{cu} (MPa)	τ_b (MPa)	$\tau_R(\sqrt{\text{MPa}})$	Mode of failure
48-NC-St-V-P1	47.98	24.12	3.48	Pullout	45-SCC-Gr-V-P3	44.88	25.03	3.74	Splitting
48-NC-St-V-P2	47.98	25.28	3.65	Pullout	45-SCC-Gr-V-P4	44.88	26.93	4.02	Splitting
48-NC-St-V-P3	47.98	27.52	3.97	Pullout	60-SCC-Gr-V-P1	59.77	26.14	3.38	Splitting
48-NC-St-V-P4	47.98	29.64	4.28	Splitting	60-SCC-Gr-V-P2	59.77	27.25	3.52	Splitting
65-NC-St-V-P1	64.65	27.41	3.41	Pullout	60-SCC-Gr-V-P3	59.77	28.39	3.67	Splitting
65-NC-St-V-P2	64.65	28.85	3.59	Pullout	60-SCC-Gr-V-P4	59.77	30.93	4.00	Splitting
65-NC-St-V-P3	64.65	29.05	3.61	Pullout	48-NC-St-N	47.98	25.90	3.74	Pullout
65-NC-St-V-P4	64.65	31.12	3.87	Splitting	65-NC-St-N	64.65	28.25	3.51	Pullout
48-NC-Gr-V-P1	47.98	18.35	2.65	Pullout	48-NC-Gr-N	47.98	21.64	3.12	Pullout
48-NC-Gr-V-P2	47.98	19.79	2.86	Pullout	65-NC-Gr-N	64.65	25.03	3.24	Splitting
48-NC-Gr-V-P3	47.98	23.48	3.39	Splitting	45-SCC-St-H-P1	44.88	26.75	3.99	Pullout
48-NC-Gr-V-P4	47.98	25.44	3.67	Splitting	45-SCC-St-H-P2	44.88	29.33	4.38	Pullout
65-NC-Gr-V-P1	64.65	24.18	3.01	Pullout	45-SCC-St-H-P3	44.88	27.41	4.09	Pullout
65-NC-Gr-V-P2	64.65	24.98	3.11	Splitting	45-SCC-St-H-P4	44.88	26.67	3.98	Pullout
65-NC-Gr-V-P3	64.65	26.03	3.24	Splitting	60-SCC-St-H-P1	59.77	30.66	3.97	Pullout
65-NC-Gr-V-P4	64.65	28.45	3.54	Splitting	60-SCC-St-H-P2	59.77	33.54	4.34	Splitting
45-SCC-St-V-P1	44.88	26.20	3.91	Pullout	60-SCC-St-H-P3	59.77	31.77	4.11	Pullout
45-SCC-St-V-P2	44.88	27.35	4.08	Pullout	60-SCC-St-H-P4	59.77	29.95	3.87	Pullout
45-SCC-St-V-P3	44.88	28.15	4.20	Pullout	45-SCC-Gr-H-P1	44.88	23.26	3.47	Pullout
45-SCC-St-V-P4	44.88	30.62	4.57	Splitting	45-SCC-Gr-H-P2	44.88	24.45	3.65	Splitting
60-SCC-St-V-P1	59.77	31.96	4.13	Pullout	45-SCC-Gr-H-P3	44.88	25.31	3.78	Splitting
60-SCC-St-V-P2	59.77	31.66	4.10	Pullout	45-SCC-Gr-H-P4	44.88	21.80	3.25	Splitting
60-SCC-St-V-P3	59.77	32.65	4.22	Pullout	60-SCC-Gr-H-P1	59.77	26.85	3.47	Splitting
60-SCC-St-V-P4	59.77	34.70	4.49	Splitting	60-SCC-Gr-H-P2	59.77	29.20	3.78	Splitting
45-SCC-Gr-V-P1	44.88	22.10	3.30	Splitting	60-SCC-Gr-H-P3	59.77	27.98	3.62	Splitting
45-SCC-Gr-V-P2	44.88	24.16	3.61	Splitting	60-SCC-Gr-H-P4	59.77	24.89	3.22	Splitting

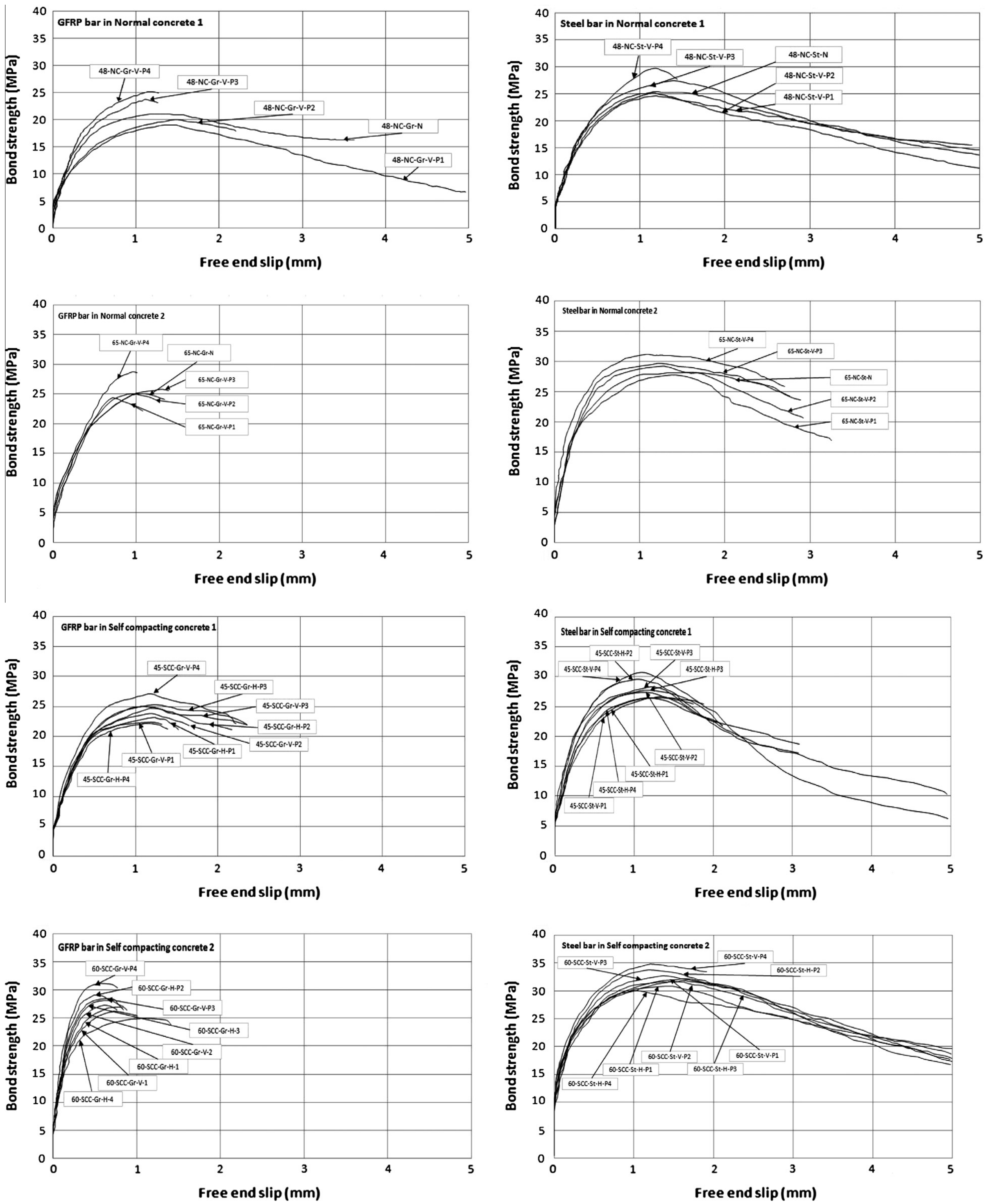

Fig. 5. Bond–slip curves of steel and GFRP bars in normal and self-compacting concretes.

in high levels of bond stress. The bond failure of GFRP bars occurred partly on the surface between concrete and resin and partly because of concrete crushing against the bar deformation. The concrete pieces that attached to the GFRP bars over the embedment length and the white powder consisting of crushed resin to the concrete cube at the location of the embedment length and the surface of GFRP bar, indicating that the interfacial bond failure occurs partly at the interface between resin and concrete and splitting failure of specimens show that crack propagation occurs in front of the bar deformation. Also, no significant damage was observed for GFRP bar deformation. This reveals that surface deformations of GFRP bars have good performance. The main reason of lower bond strength of GFRP bars compared to steel bars is because of their weaker surface treatment that could not supply enough adhesion with concrete. The splitting failure of GFRP bars in concrete compared to the pullout failure of steel bars in the same concrete shows that propagation of splitting cracks of GFRP bars is higher than steel bars in surrounding concrete and it could be because of its lower modulus of elasticity.

3.2. Bond strength in horizontal casting specimens

Fig. 7 shows the variation of normalized bond strength of steel and GFRP bars in SCC for horizontally casting specimens. For NC1, normalized bond strength for steel bars was 3.74 in the case of 200 × 200 × 200 mm pullout specimens; while that for NC2 was 3.51. For NC1, normalized bond strength for GFRP bars was 3.12 in the case of 200 × 200 × 200 mm pullout specimens; while that for NC2 was 3.24. In the case of SCC1, normalized bond strength for steel bars ranges between 3.98 and 4.38 across the length of the specimens from right to left (Fig. 2); while those for SCC2 ranges between 3.87 and 4.34. For SCC1, normalized bond strength for GFRP bars ranges between 3.25 and 3.78 across the length of the specimens from right to left; while those for SCC2 ranges between 3.22 and 3.78. Bond strengths are higher at the middle bars compared to bars at both extremities. This could be due to the uniform mixture in the middle parts of horizontal specimens. The average normalized bond strength of steel and GFRP bars in SCC was higher than those in NC. This is because of the superior filling capacity of SCCs. The average normalized bond strength of steel bars in SCC is 12.83% higher than those in NC. Also, this is 15.89% higher than GFRP bars in SCC. The normalized bond strength of GFRP bars in SCC is 10.98% higher than those in NC. Also for SCC, the average drop of normalized bond strength of steel bars across the length of the specimens from right to left is 10.98%, while those for GFRP bars is 16.71%.

3.3. Bond strength in vertical casting specimens

Fig. 8 presents the normalized bond strength of steel and GFRP bars in both NC and SCC specimens at different heights. For NC1, normalized bond strength for steel bars ranges between 3.48 and 4.28 across the length of the specimens from top to bottom; while those for NC2 ranges between 3.41 and 3.87. For NC1, normalized bond strength for GFRP bars ranges between 2.65 and 3.67 across the length of the specimens from top to bottom; while those for

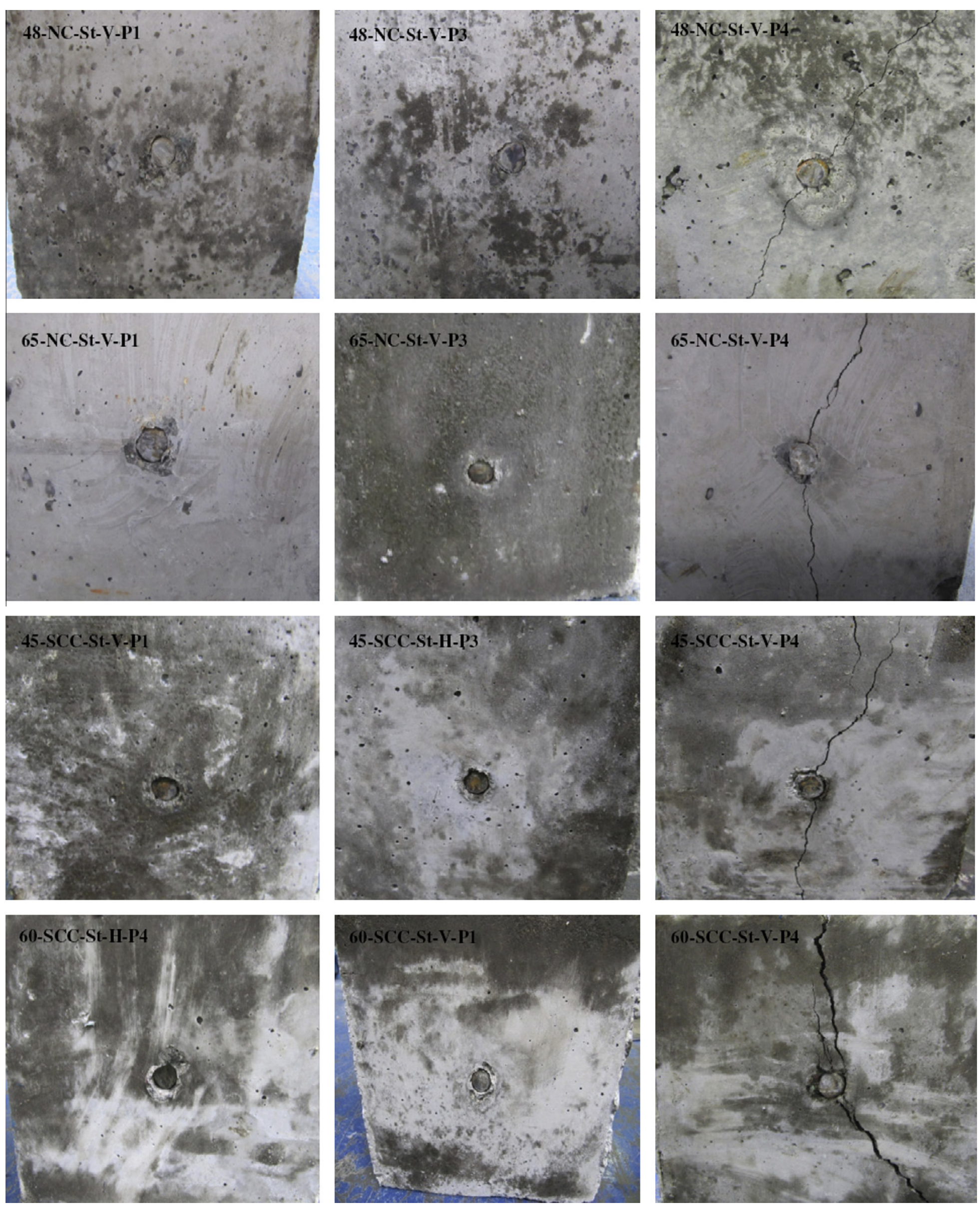

Fig. 6. Interfacial bond failure of some steel bars in normal and self-compacting concretes.

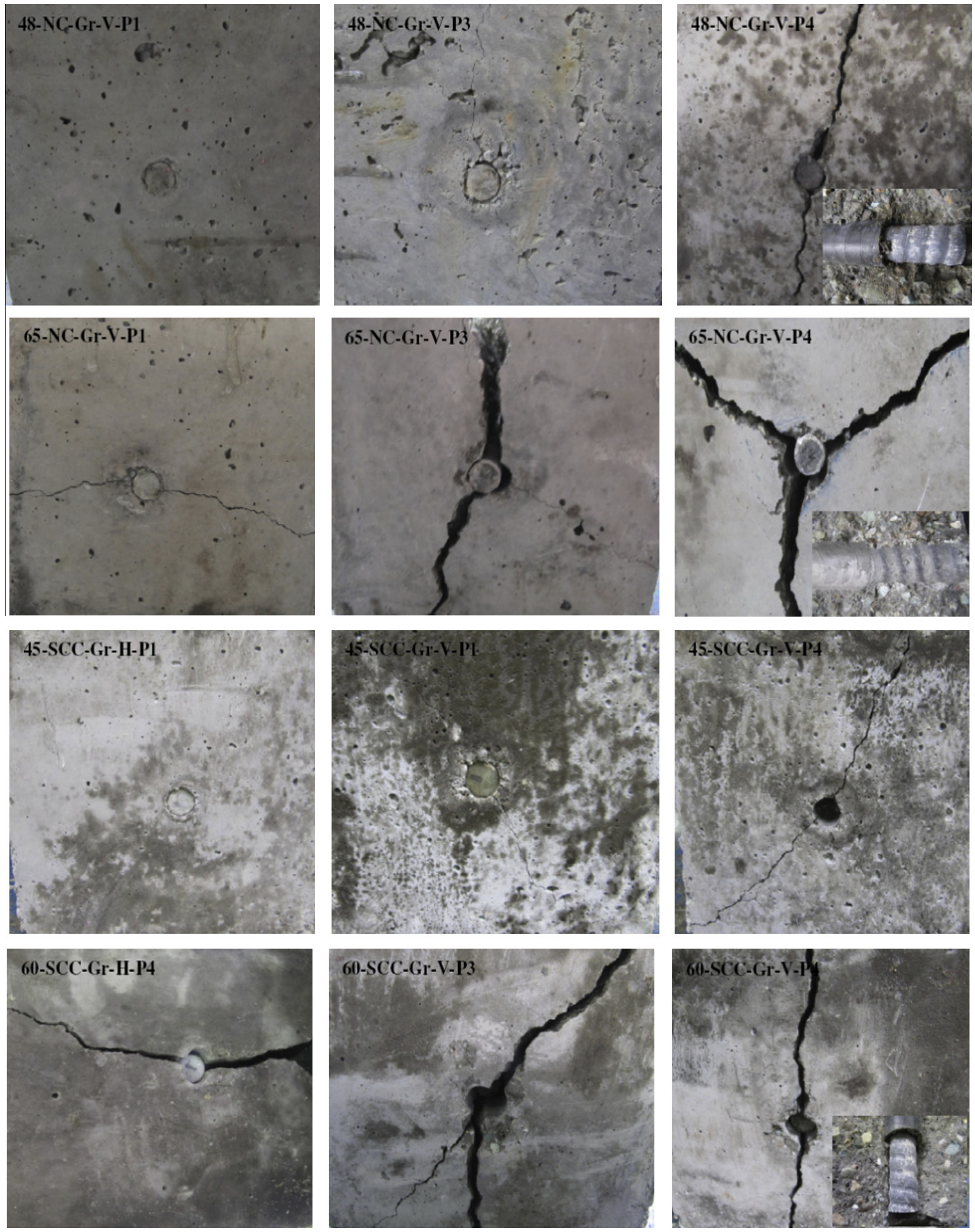

Fig. 6 (*continued*)

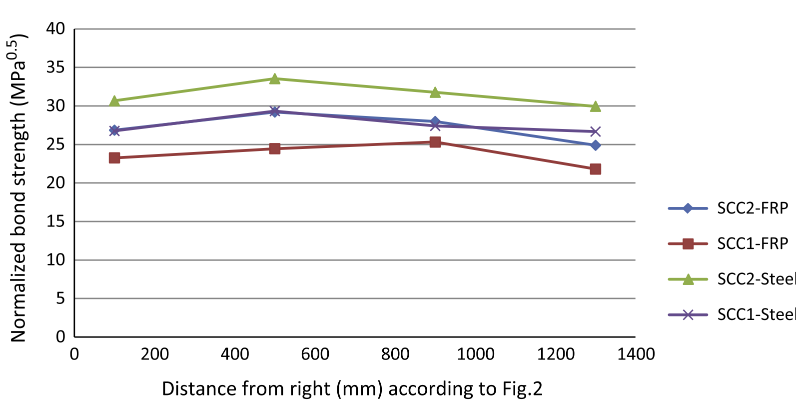

Fig. 7. Normalized bond strength of steel and GFRP bars in horizontal casting specimens.

NC2 ranges between 3.00 and 3.54. For SCC1, normalized bond strength for steel bars ranges between 3.91 and 4.57 across the length of the specimens from top to bottom; while those for SCC2 ranges between 4.13 and 4.49. For SCC1, normalized bond strength for GFRP bars ranges between 3.30 and 4.02 across the length of the specimens from top to bottom; while those for

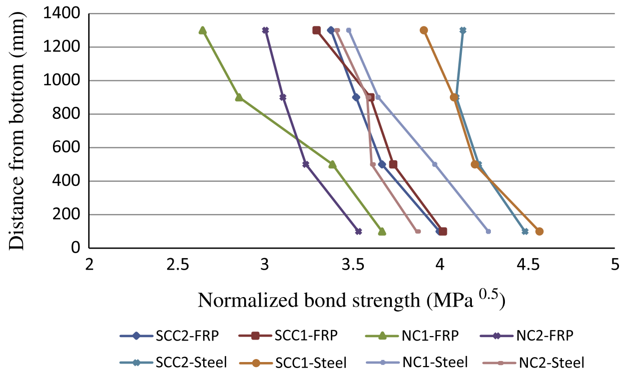

Fig. 8. Normalized bond strength of steel and GFRP bars in vertical casting specimens.

SCC2 ranges between 3.38 and 4.00.For both SCC and NC, bond strength in the bottom bars are higher than those in top bars. The variations of normalized bond strength of steel and GFRP bars in SCC are lower than those of NC. Meanwhile, for both concretes, the average bond strength in height is higher for a steel bar as compared to a GFRP bar.

The losses of bond strength with height are shown in Fig. 9. As shown in this figure, the average drop in bond strength of steel bars between the upper and lower zones of the columns is about 12.72% in SCC and 18.21% in NC. Also, for a GFRP bar, the drop in bond strength between the upper and lower zones of the columns is about 20.09% in SCC and 28.15% in NC. In accordance with these results; the drop in bond strength of steel bars at the top of the columns averages 5.49% less in SCC than in NC and 8.06% in the case of GFRP bars. Several standards for NC set the loss of bond strength of steel bars in top bars at 30%; which is not matched to 18.21% in this study. Statistical analysis indicates that in NC, with a low water to cement ratio and high cementitious material, the anchorage length of top steel bars could be 18.21% higher than the bottom ones. Also, in the case of SCC, this increscent is 12.72%. Meanwhile, the anchorage length of top GFRP bars in NC and SCC could be 28.15% and 20.09% higher than the bottom ones, respectively.

3.4. Performance of code based and other existing bond equations

Various bond tests and formulas have been developed for predicting the bond strength of steel and GFRP bars in concrete. Regardless of the bond failure mechanism and concrete type, the performance of some equations in the prediction of bond strength of deformed bars embedded in various NC and SCC mixtures is investigated as below:

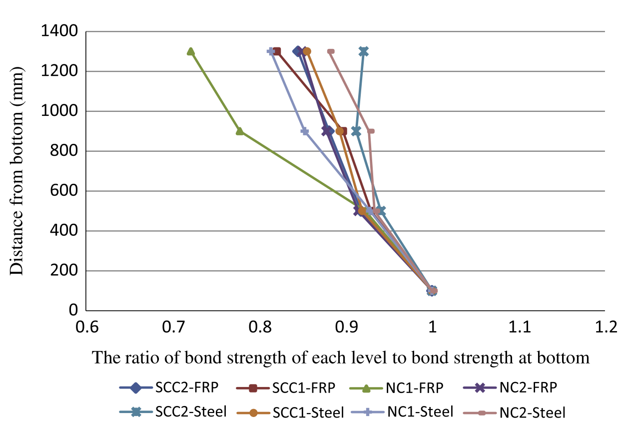

Fig. 9. The ratio of bond strength of each level to bond strength at bottom for different bar and concrete.

Orangun et al. [38] developed expressions to describe the bond strength of steel bars with and without confining transverse reinforcement. For bars not confined by transverse reinforcement, a regression analysis was used to produce the following expression for the average bond stress at failure:

$$\tau_b = \left(0.10 + 0.25\frac{c_{\min}}{d_b} + 4.15\frac{d_b}{l_d}\right)(f_c')^{0.5} \quad (3)$$

in which $c_{\min}$ and f_c' are the minimum cover of bar and specified compressive strength of concrete, respectively.

Darwin et al. [39] used a large database for the bond strength prediction of steel bars. Based on their studies, the best-fit equation for the bond strength of steel bars not confined by transverse reinforcement was as follows:

$$\tau_b = [1.5l_d(c_{\min} + 0.5d_b) + 51A_b]\left(0.1\frac{c_{\max}}{c_{\min}} + 0.90\right)\left(f_c'^{1/4}\right)(\pi d_b l_d)^{-1} \quad (4)$$

where $c_{\max}$ is the maximum of (bottom concrete cover of reinforcing bar) and (the minimum of side concrete cover for reinforcing bar and half of the bar clear spacing plus 6.35 mm) and A_b is the area of reinforcing bar.

Zuo and Darwin [40] developed their descriptive equation for steel bars not confined by transverse reinforcement as follows:

$$\tau_b = [1.43l_d(c_{\min} + 0.5d_b) + 56.2A_b]\left(0.1\frac{c_{\max}}{c_{\min}} + 0.90\right)\left(f_c'^{1/4}\right)(\pi d_b l_d)^{-1} \quad (5)$$

ACI design code [41] presented the following equation for the prediction of the bond strength of steel bars in concrete:

$$\tau_b = [1.43l_d(c_{\min} + 0.5d_b) + 57.4A_b]\left(0.1\frac{c_{\max}}{c_{\min}} + 0.90\right)\left(f_c'^{1/4}\right)(\pi d_b l_d)^{-1} \quad (6)$$

Chapman and Shah [42] proposed Eq. (7) which compares satisfactorily with the test data in which all three types of failures (pull-out, splitting of concrete, and yielding of steel) were included:

$$\tau_b = \left(0.29 + 0.282\frac{c_{\min}}{d_b} + 4.734\frac{d_b}{l_d}\right)(f_c')^{0.5} \quad (7)$$

Lee et al. [29] investigated the influence of the compressive strength of concrete on the bond strength of the steel and GFRP bars as a function of concrete strength up to 90 MPa based on the experimental results. The following equations are presented for bond prediction of steel and GFRP bars in concrete, respectively.

$$\tau_b = 4.1(f_c')^{0.5} \quad (8)$$

$$\tau_b = 3.3(f_c')^{0.3} \quad (9)$$

ACI design code and CEB-FIP model code adopt a concept in which the bond strength of GFRP bars increases in proportion to the concrete tensile strength, which is related to the square root of the compressive strength of concrete. According to the ACI design code and CEB-FIP model, the bond strength of GFRP bars in concrete is determined using the following equations, respectively:

$$\tau_b = 20.23\frac{\sqrt{f_c'}}{d_b} \quad (10)$$

$$\tau_b = 13.50\left(\frac{f_c'}{30}\right)^{\beta} \quad (11)$$

In the latter equation, β is the coefficient related to f_c' ($\beta = 1/2$ has been adopted in CEB-FIP code for the τ_b in case of "good" bond conditions).

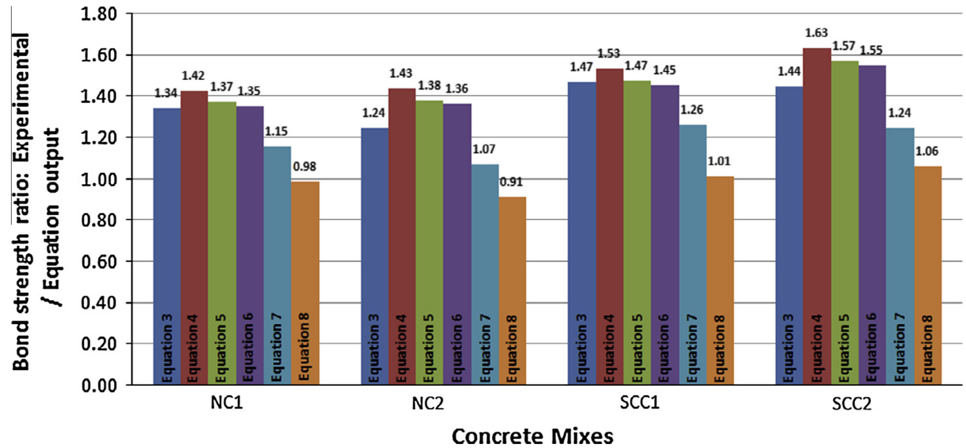

Fig. 10. Comparative performance of bond equations for steel bars in concrete.

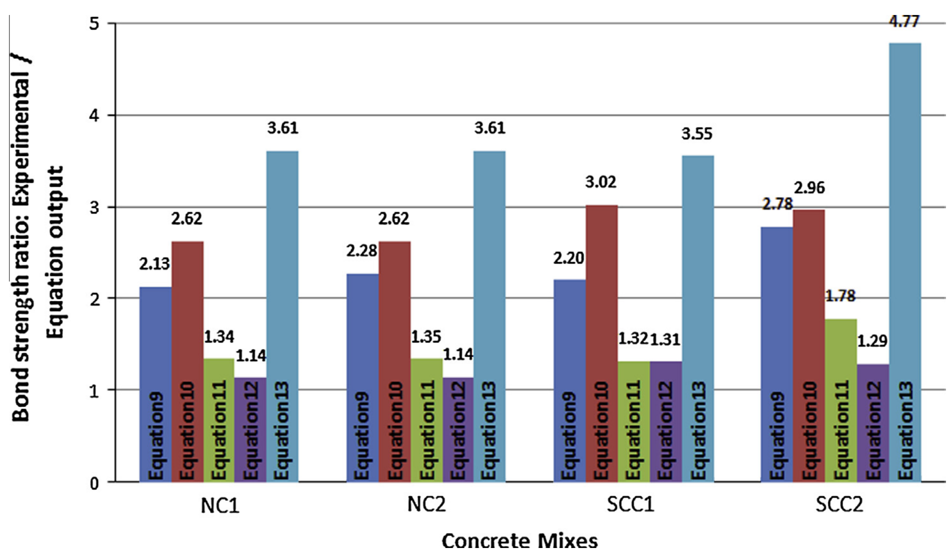

Fig. 11. Comparative performance of bond equations for GFRP bars in concrete.

The American Concrete Institute (ACI) [43] presented a linear regression of the normalized average bond stress of GFRP bars versus the normalized cover and embedment (splice) length according to the following relationship after rounding the coefficients:

$$U = \left(4.0 + 0.3\frac{c_{\min}}{d_b} + 100\frac{d_b}{l_d}\right)\left(0.083\sqrt{f_c'}\right) \tag{12}$$

Okelo and Yuan [27] proposed Eq. (13) based on 151 test specimens containing 6, 8, 10, 16, and 19 mm GFRP bars embedded in a 203 mm concrete cube for different compressive strengths of concrete (29–60 MPa). The average bond strength of GFRP bars was proportional to the square root of concrete compressive strength.

$$\tau_b = 14.70\frac{\sqrt{f_c'}}{d_b} \tag{13}$$

In this section, the performance of all these equations in the bond strength prediction of steel and GFRP bars embedded in various SCC and NC mixtures was investigated. The performances of these equations were described by the experimental to theoretical bond strength ratio as presented in Figs. 10 and 11.

For equations that predict the bond strength of steel bars in concrete, as shown in Fig. 10, Eq. (8) overestimates the bond strength inconsiderably; however, this equation is closely adapted for the bond strength prediction of steel bars in SCC. All other equations underestimate the bond strength of steel bars. Eq. (4) highly under-predicts the bond strength of steel bars in concrete. Meanwhile, Eq. (7) is more suitable for the bond strength prediction of steel bars in NC compared to other equations.

In the case of bond strength prediction of GFRP bars in concrete, as shown in Fig. 11, all equations underestimate the bond strength. However Eq. (13) significantly under-predicts the bond strength of steel bars in concrete and Eq. (12) is more appropriate for bond strength prediction of GFRP bars in NC and SCC compared to other equations.

4. Conclusion

The bond behavior of steel and GFRP bars in normal and self-compacting concretes were investigated in this study. The variations of bond strength of reinforcing bars in the length of horizontal and vertical specimens were scrutinized. On the basis of the analysis and comparison of the test results of 104 pullout specimens, the following observations and conclusions can be made:

(1) Higher bond strength and linear bonding behavior of steel bars at the beginning of loading indicates that their adhesion behavior is better than GFRP bars in both normal and self-compacting concretes.
(2) The splitting failure of GFRP bars in both normal and self-compacting concretes compared to the pullout failure of steel bars in the same concretes show that the propagation of splitting cracks of GFRP bars is higher than steel bars in concrete.
(3) The bond strengths of steel and GFRP bars in self-compacting concrete are higher at the middle bars compared to bars at both extremities. This could be because of uniform mixture in the middle parts of horizontal specimens.
(4) For horizontal specimens, the average normalized bond strength of steel and GFRP bars in SCC is 12.83% and 10.98% higher than those in NC, respectively. This is due to the superior filling capacity of SCC compared to NC.
(5) In the case of horizontal specimens, the average normalized bond strength of steel bars is 15.89% higher than GFRP bars in SCC. This is due to the better treatment of steel bars and SCC compared to GFRP bars (i.e. higher chemical adhesion and modulus of elasticity of steel bars).
(6) For horizontal specimens, the average drop of normalized bond strength of steel bars across the length of the specimens from right to left is 10.98%, while those for GFRP bars is 16.71%. This shows the variations of bond strength of steel bars in SCC being less than GFRP bars.
(7) For vertical specimens, using low water to cement ratio and high cementitious material for NC could decrease the difference of anchorage length of top steel bars and bottom ones. The average anchorage length of top steel bars in normal concrete (that is used in this investigation) is 18.21% higher than bottom ones.
(8) In the case of vertical specimens, the anchorage length of top steel bars in SCC is lower than that in NC. The anchorage length of top steel bars in SCC is 12.72% higher than bottom ones in this study. The anchorage length of top GFRP bars in NC and SCC could be 28.15% and 20.09% higher than bottom ones, respectively.
(9) Comparing different equations regarding the bond prediction of steel and GFRP bars in concrete, shows that the equation proposed by Chapman and Lee are suitable for the bond strength prediction of steel bars in normal and self-compacting concretes, respectively; while the equation proposed by ACI 440 is appropriate for the bond strength prediction of GFRP bars in both normal and self-compacting concretes.

References

[1] Ozawa K, Maekawa K, Kunishima H, Okamura H. Performance of concrete based on the durability design of concrete structures. In: Proceedings of second East Asia-Pacific conference of Struct Eng Const. 1989. p. 445–56.
[2] Skarendahl A. Self-compacting concrete for improved productivity, working environment and performance. In: Paper presented at IREX Meeting, Réuniond'informationsur les bétonsautoplacants, Paris; 1999.
[3] Sonebi M, Batros P, Zhu W, Gibbs J, Tamimi A. Properties of hardened concrete. Task 4, final report, Advance Concrete Masonry Center, University of Paisley, Scotland, UK; 2000. p. 6–73.
[4] Campion MJ, Jost P. Self-compacting concrete. Concr Int: Des Constr 1999;22:31–4.
[5] Khayat KH, Manai K, Trudel A. In situ mechanical properties of wall elements using self-consolidating concrete. ACI Mater 1997;94(6):491–500.
[6] Yurugi M. Application of self-compacting concrete in Japan. In: Proceedings of 23rd OWICS conference, CI-Premier Ptc Ltd, Singapore; 1998. p. 29–42.
[7] Petersson O. Application of self-compacting concrete for bridge castings. Swed Cem Concr Res Inst 1998;54(2).
[8] Arima I, Takeguchi M, Sakurai S, Hayashi J. The quality of super workable concrete used for the construction of Akashi-Kaikyo Bridge 4A anchorage. Proc Jpn Concr Inst 1994;16(1):25–30.
[9] Domone PL. Self-compacting concrete: an analysis of 11 years of case studies. Cement Concr Comp 2006;28(2):197–208.
[10] Domone PL. A review of the hardened mechanical properties of self-compacting concrete. Cement Concr Comp 2007;29(1):1–12.
[11] Aiello MA, Leone M, Pecce M. Bond performance of FRP rebars-reinforced concrete. Mater Civ Eng J 2007;19(3):205–13.
[12] Tepfers R. A theory of bond applied to overlapped tensile reinforcement splices for deformed bars. Division of Concrete Structures, Chalmers University of Technology of Goteborg; 1973.
[13] Tepfers R, Lorenzis LD. Bond of FRP reinforcement in concrete – a challenge. J Mech Compos Mater 2003;39(4):477–96.
[14] Petrov N, Khayat KH, Tagnit- Hamou A. Effect of stability of self consolidating concrete on the distribution of steel corrosion characteristics along experimental wall elements. In: Ozawa K, Ouchi M, editors. Proceedings of second international RILEM symposium on self-compacting concrete. Tokyo: 2001. p. 441–50.
[15] Tragardh J. Microstructural features and related properties of self compacting concrete. In: Skarendhal A, Petersson O, editors. Proceedings of first international RILEM symposium on self compacting concrete. Stockholm; 1999. p. 175–186.
[16] Zhu W, Bartos PJM. Microstructure and properties of interfacial transition zone in SCC. In: Yu Z, Shi C, Khayat KH, Xie Y, editors. Proceedings of first international symposium on design, performance and use of self-consolidating concrete. China: Changsha; 2005. p. 319–27.
[17] Bentur A, Diamond S, Minders S. Cracking process in steel fiber reinforced cement paste. Cement Concr Res 1985;15(2):331–42.
[18] Leemann A, Munch B, Gasser P, Holzer L. Influence of compaction on the interfacial transition zone and the permeability of concrete. Cement Concr Res 2006;36(8):1425–33.
[19] Schiessl A, Zilch K. The effects of the modified composition of SCC on shear and bond behaviour. In: Ozawa K, Ouchi M, editors. Proceedings of second international RILEM symposium on self compacting concrete. Tokyo; 2001. p. 501–6.
[20] Chan YW, Chen YG, Liu YS. Development of bond strength of reinforcement steel in self-consolidating concrete. ACI Struct J 2003;100(4):490–8.
[21] Castel A, Vidal T, Viriyametanont K, Francois R. Effect of reinforcing bar orientation and location on bond with self-consolidating concrete. ACI Struct J 2006;103(4):559–67.
[22] Valcuende M, Parra C. Bond behaviour of reinforcement in self compacting concretes. Constr Build Mater 2009;23:162–70.
[23] Khayat KH. Use of viscosity-modifying admixture to reduce top-bar effect of anchored bars cast with fluid concrete. ACI Mater J 1998;95(2):158–67.
[24] Esfahani MR, Lachemi M, Kianoush MR. Top-bar effect of steel bars in self-consolidating concrete (SCC). Cement Concrete Comp 2008;30(1):52–60.
[25] Bank LC, Puterman M, Katz A. The effect of material degradation on bond properties of fiber reinforced plastic reinforcing bars in concrete. ACI Mater J 1998;95(3):232–43.
[26] Achillides Z, Pilakoutas K. Bond behavior of fiber reinforced polymer bars under direct pullout conditions. J Compos Const 2004;8(2):173–81.
[27] Okelo R, Yuan LR. Bond strength of fiber reinforced polymer rebars in normal strength concrete. J Compos Const 2005;9(3):203–13.
[28] Wambeke BW, Shield CK. Development length of glass fiber-reinforced polymer bars in concrete. ACI Struct J 2006;103(2):11–7.
[29] Lee JY, Kim TY, Kim TJ, Yi CK, Park JS, You YC, et al. Interfacial bond strength of glass fiber reinforced polymer bars in high-strength concrete. Compos Part B: Eng 2008;39:258–70.
[30] Davalos JF, Chen Y, Ray I. Effect of FRP bar degradation on interface bond with high strength concrete. Cement Concr Compos 2008;30:722–30.
[31] Katz A, Berman N. Modeling the effect of high temperature on the bond of FRP reinforcing bars to concrete. Cement Concr Compos 2000;22:433–43.
[32] Wona JP, Park CG, Kim HH, Lee SW, Jang CI. Effect of fibers on the bonds between FRP reinforcing bars and high-strength concrete. Compos Part B: Eng 2008;39:747–55.
[33] Khayat KH, Bickley J, Lessard M. Performance of self-consolidating concrete for casting basement and foundation walls. ACI Mater J 2000;97(3):374–80.
[34] Nagataki S, Fujiwara H. Self-compacting property of highly flowable concrete. SP-154, ACI; 1995. p. 301–14.
[35] Ozawa K, Sakata N, Iwai M. Evaluation of self compactibility of fresh concrete using funnel test. In: Proceeding of JSCE; 1994. p. 490.
[36] European Project Group. Specification and guidelines for self-compacting concrete. European Federation for Specialist Construction Chemicals and Concrete Systems, UK: EFNARC; 2002.
[37] Xial J, Falkner H. Bond behavior between recycled aggregate concrete and steel rebars. Constr Build Mater 2007;21:395–401.
[38] Orangun CO, Jirsa JO, Breen JE. Reevaluation of test data on development length and splices. ACI Mater J 1977;74(3):114–22.
[39] Darwin D, Tholen ML, Idun EK, Zuo J. Splice strength of high relative rib area reinforcing bars. ACI Struct J 1996;93(1):95–107.
[40] Zuo J, Darwin D. Splice strength of conventional and high relative rib area bars in normal and high-strength concrete. ACI Struct J 2000;97(4):630–41.
[41] ACI 408R. Bond and Development of Straight Reinforcing Bars in Tension. American Concrete Institute; 2003. p. 49.
[42] Chapman RA, Shah SP. Early-age bond strength in reinforced concrete. ACI Mater J 1988;84(6):501–10.
[43] ACI 440.1R. Guide for the Design and Construction of Structural Concrete Reinforced with FRP Bars. American Concrete Institute; 2006. p. 44.